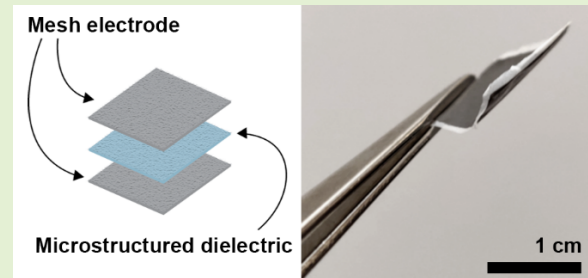


# Inkjet-Printed, Nanofiber-Based Soft Capacitive Pressure Sensors for Tactile Sensing

Riikka Mikkonen<sup>1</sup>, Anastasia Koivikko<sup>2</sup>, Tiina Vuorinen<sup>1</sup>, Veikko Sariola<sup>1</sup>, *Member, IEEE*,  
and Matti Mäntysalo<sup>1</sup>, *Member, IEEE*

**Abstract**—The development of soft electronics is critical to the realization of artificial intelligence that comes into direct contact with humans, such as wearable devices, and robotics. Furthermore, rapid prototyping and inexpensive processes are essential for the development of these applications. We demonstrate here an additive, low-cost method for fabricating polydimethylsiloxane based soft electronics by inkjet printing. Herein, a novel approach using a water-soluble polyvinyl alcohol layer as the substrate, inexpensive, fully digital fabrication of capacitive pressure sensors is enabled by sandwiching mesh-like conductive layers and microstructured dielectric in a straightforward, convenient manner. These sensors exhibit improved sensitivity ( $4 \text{ MPa}^{-1}$ ) at low pressures ( $<1 \text{ kPa}$ ) in contrast to sensors with a flat elastomer dielectric and can still detect large pressures around  $50 \text{ kPa}$ , having excellent long-term repeatability over 2000 cycles, without significant hysteresis ( $\leq 8.5\%$ ). The tactile sensing ability of the fabricated devices was demonstrated in a practical application. Moreover, sensor characteristics are easily adjustable, simply by changing printing parameters or tuning the ink solution. The proposed approach provides scalable solution for fabricating high-sensitivity printed sensors for e-skin and human-machine interfaces.

**Index Terms**—Polydimethylsiloxane, capacitive pressure sensor, inkjet printing, printed electronics, soft electronics, polyvinyl alcohol.



## I. INTRODUCTION

SOFT and flexible electronics have been of interest in the recent years for their promising applications in human-machine interfaces, skin prosthetics, soft robotics, and wearable electronics [1]–[6]. These devices should be both flexible and lightweight. Additionally, high sensitivity, robustness and ease of fabrication are desirable characteristics for soft electronics.

Manuscript received December 1, 2020; revised March 30, 2021; accepted May 4, 2021. Date of publication May 31, 2021; date of current version November 30, 2021. This work was supported in part by the Academy of Finland under Grant 299087 and Grant 310618 and in part by the Academy of Finland funded Research Infrastructure “Printed Intelligence Infrastructure” (PII-FIRI) under Grant 320019. The work of Riikka Mikkonen was supported by Walter Ahlström Foundation. The work of Anastasia Koivikko was supported by the Finnish Science Foundation for Technology and Economics. This article was presented at the 2020 IEEE International Conference on Flexible and Printable Sensors and Systems (FLEPS). The associate editor coordinating the review of this article and approving it for publication was Dr. Luigi Occhipinti. (*Corresponding author: Riikka Mikkonen.*)

Riikka Mikkonen, Tiina Vuorinen, and Matti Mäntysalo are with the Faculty of Information Technology and Communication Sciences, Tampere University, 33104 Tampere, Finland (e-mail: riikka.mikkonen@tuni.fi; matti.mantysalo@tuni.fi).

Anastasia Koivikko and Veikko Sariola are with the Faculty of Medicine and Health Technology, Tampere University, 33104 Tampere, Finland.

This article has supplementary downloadable material available at <https://doi.org/10.1109/JSEN.2021.3085128>, provided by the authors.

Digital Object Identifier 10.1109/JSEN.2021.3085128

In the skin-like electronics and other wearable applications, pressure sensing is one important function. Typical pressure sensors are often capacitive [7], piezoresistive [8], piezoelectric [9] or triboelectric [10]. The capacitive sensors are a popular choice for their structural simplicity, ease of fabrication, tunability and low power consumption [11]–[13]. A typical structure of the capacitive-type soft sensor consists of a dielectric layer, typically an elastomer, sandwiched between two flexible electrodes. Such sensors are essentially plate capacitors, and thus their performance is heavily influenced by choice of the dielectric material. Therefore, great attention has been paid to the dielectric characteristics.

Among elastic materials, soft silicone elastomers, especially polydimethylsiloxane (PDMS) is an interesting option for many wearable applications for being inexpensive, transparent, inert, biocompatible with human tissues and mechanically resilient [14]–[17]. Furthermore, PDMS properties can be tuned simply by changing the cross-linking ratio of the prepolymer and the curing agent; a low cross-linking density makes the elastomer more gel-like, whereas the elastic properties are more dominant with a higher cross-linking density. However, it has been shown that the viscoelastic characteristics of the soft elastomer also might have a significant effect on, for example, the hysteresis and sensitivity of soft sensors [18].

Dielectric layers with microstructures, such as pores and pyramids, have been used to improve the sensitivity and to

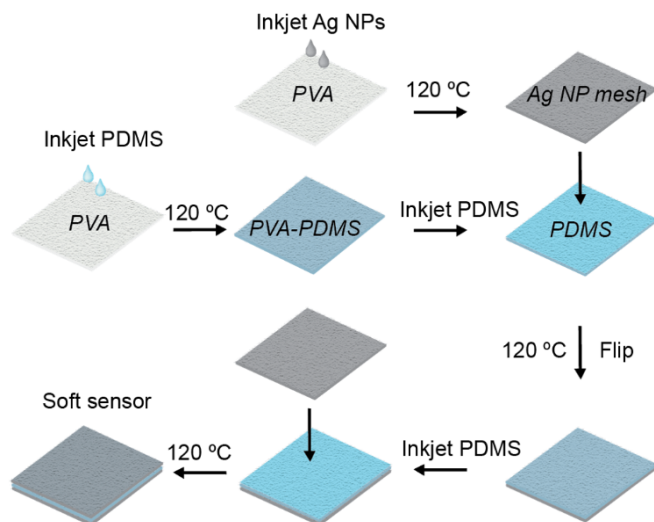


Fig. 1. Schematic illustration of sensor fabrication process.

reduce hysteresis of the sensor, because these microstructures may be more easily compressed than flat films [14], [19]–[23]. Many such microstructures are fabricated by using lithographic methods, in which cumbersome, time-consuming processes and hazardous chemicals are used [13], [20], [21].

To address these issues, additive fabrication techniques, like printing technologies have been used [7], [24]–[26]. Printed electronics have attracted increasing attention in recent years as an alternative to conventional microfabrication technologies to realize a range of low-cost, large-area, and flexible functional devices. Especially the fully additive methods, such as inkjet printing, offer mask-free, cost-effective, and digital methods to fabricate functional patterns in large scale, in comparison with other methods used to assemble material layers into electronic devices, such as spin-coating and lithographic patterning [27]–[29].

In this work, we report a facile method for fabricating fully printed, elastomeric capacitive sensors with high flexibility and great sensitivity at a wide pressure range. Earlier, we developed an inkjet printable PDMS solution for multilayer printing of soft electronics [30], and the process was further studied in [31]. However, challenges remained in the realization of uniform conductive layer with good adhesion on top of the printed PDMS layer in these studies. In addition, fabrication of self-standing printed PDMS layers, or the options for transferring the printed structures to the target substrate were not addressed before.

Here, we have solved these issues by using water-soluble, electrospun polyvinyl alcohol (PVA) fibers both as a temporary carrier and a functional layer, to realize fully inkjet printed tactile pressure sensors. It has been shown earlier that this material can be used to improve not only the mechanical strength and elasticity of soft, skin-like electronics, but also skin-mountability and wear comfort [32]–[34].

We fabricated conductive mesh electrodes by inkjet printing silver nanoparticles (Ag NP) on PVA, while a dielectric layer, consisting of a PVA mesh layer embedded in an inkjet printed PDMS layer, was placed between the mesh electrodes to form a capacitive tactile pressure sensor. Two different PDMS cross-linking densities were used to compare the impact of

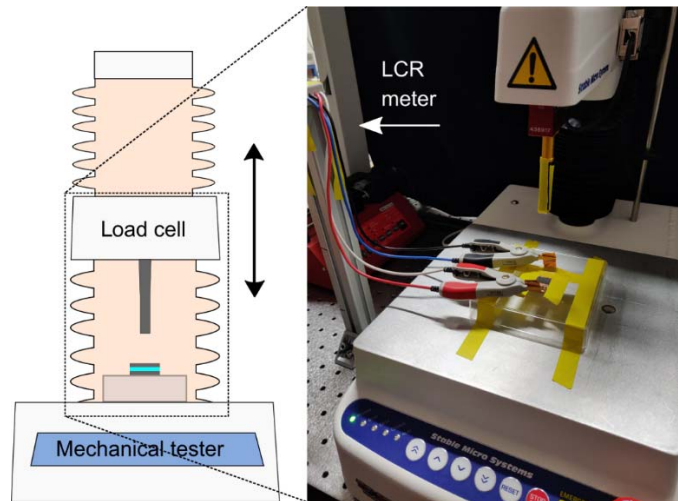


Fig. 2. Experimental setup for measuring the change in capacitance in response to applied pressure, including a schematic illustration of the sample placed to a mechanical tester, together with a photograph of a sample attached to the tester and connected to the LCR meter.

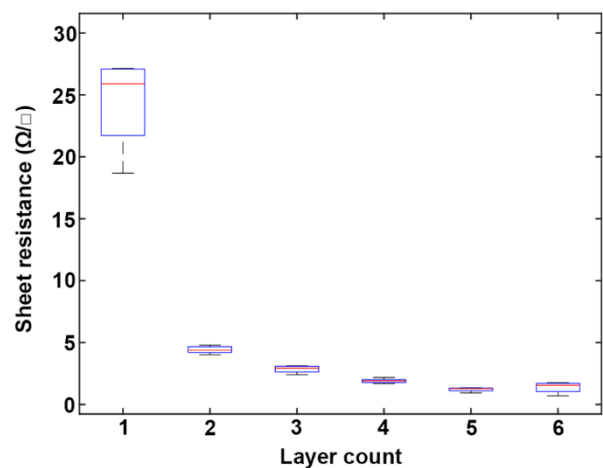


Fig. 3. Sheet resistances of the Ag NP prints as a function of layer count. Boxplot is showing the interquartile range of 5 measurements, and the whiskers show the whole range of the measured values.

the viscoelasticity on the sensor performance. These printed sensors were characterized in comparison to reference sensors with conventional, spin-coated dielectric layers.

## II. MATERIALS AND METHODS

### A. Sensor Fabrication Process

1) *The PVA-Layer*: PVA solution was prepared by dissolving PVA granules in deionized (DI) water. The used PVA material had molecular weight of 47000 with a degree of hydrolysis of 98.0 – 98.8 mol% (Fluka, Germany). Then, the PVA-layer was electrospun using KDS 100 syringe infusion pump (kdScientific, USA) together with Chargemaster high voltage supply (SIMCO, USA). Electrospinning was done with 2 ml/h feeding speed and 25 cm distance and 25 kV voltage between the needle and the substrate.

2) *Inkjet-Printing of the Mesh Electrodes*: The PVA layer was carefully peeled from the electrospinning substrate and placed on a hydrophobic ethylene tetrafluoroethylene (ETFE)-substrate (Novoflon ET 6235 EZ, NOVOFOL Kunststoffprodukte GmbH & Co, Germany). Ag NP ink (DGP 40LT-15C, Advanced Nanoproducts, Korea) was used for

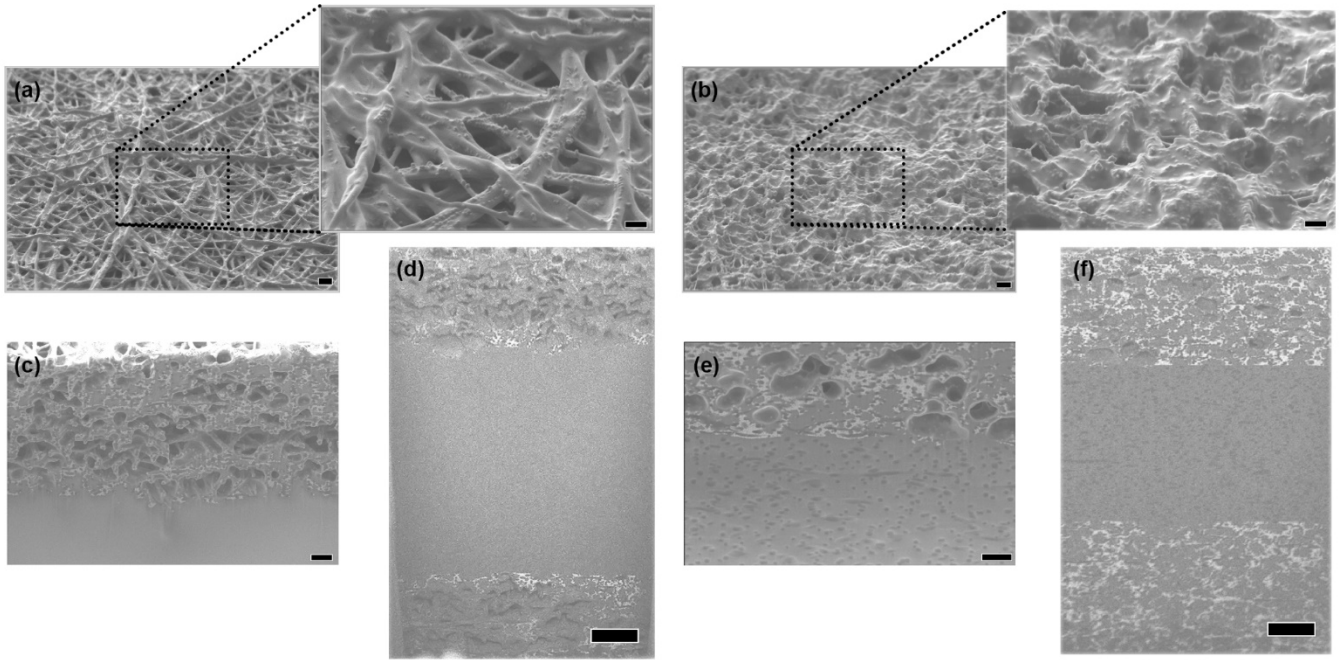


Fig. 4. SEM-images of the fabricated sensors showing (a) the surface of the reference sensor's mesh electrode, scale bar  $1\ \mu\text{m}$  (inset  $500\ \text{nm}$ ), (b) surface of the printed sensor's mesh electrode, scale bar  $1\ \mu\text{m}$  (inset  $500\ \text{nm}$ ), (c) interface between the reference sensor's electrode and the spin-coated dielectric, scale bar  $1\ \mu\text{m}$ , (d) cross-section of the reference sensor: the spin-coated dielectric is sandwiched between the electrodes, scale bar  $3\ \mu\text{m}$  (e) interface between the printed sensor's electrode and the printed PVA-PDMS dielectric, scale bar  $1\ \mu\text{m}$ , (f) cross-section of the printed sensor: the printed PVA-PDMS dielectric is sandwiched between the electrodes, scale bar  $3\ \mu\text{m}$ .

inkjet printing the electrode pattern on the PVA mesh with a Dimatix DMP-2831 material printer (Fujifilm, USA). After printing, the electrodes were thermally cured at  $120\ ^\circ\text{C}$  for 60 min.

3) *Inkjet Printing of the PDMS Dielectric*: The sensor dielectric was fabricated by inkjet printing PDMS onto the PVA mesh. Sylgard 184 (Dow, USA) was selected as the dielectric material since its printability has been demonstrated in our earlier work [30]. Here, two cross-linking densities of the PDMS were used: stiffer (1:10), and softer (1:20) (curing agent to base-ratio). The PDMS was diluted in octyl acetate in a 1:3 weight ratio to allow printing without cartridge heating using the Dimatix DMP-2831 material printer. These freshly printed dielectric layers were thermally cured at  $120\ ^\circ\text{C}$  for 25 min. For comparison, reference dielectrics were fabricated by spin-coating (4000 rpm, 60 s) thin foils of Sylgard 184 in both 1:10 and 1:20 ratio on top of an ETFE substrate.

4) *Stacking the Device*: After curing the dielectric, additional PDMS layers were printed to make a wet, glue-like layer, onto which the bottom electrode was placed and gently pressed to bond the layers. Excessive ink was wiped from the surface, and the whole structure was thermally cured at  $120\ ^\circ\text{C}$  for 25 min. After attaching the bottom electrode, the whole device was turned upside down, and the process was repeated to add the top electrode. Again, the device was cured at  $120\ ^\circ\text{C}$  for 25 min to bond the material layers. Finally, the remnants of the PVA layers were dissolved with DI water. A similar process was used to stack the reference devices with the spin-coated PDMS dielectrics, but instead of printing,  $1\ \mu\text{l}$  of the ink solution was dispensed with a pipette to form the glue-like layer for bonding the electrodes. A visual presentation of the sensor fabrication process is given in Fig. 1.

## B. Characterization

1) *Electrical Properties of the Mesh Electrode*: The resistance of the Ag NP mesh with increasing layer count was measured with a multimeter. The sheet resistance  $R_s$  of each sample was calculated from the measured resistance value with the following formula:

$$R_s = R \frac{w}{l} \quad (1)$$

where  $l$  is the line length and  $w$  is the width of the conductive line.

2) *Cross-Sectional Imaging (FIB SEM)*: A high-resolution scanning electron microscope with a FIB (Crossbeam 540, Zeiss) was used for the cross-sectional imaging of the devices.

3) *Pressure-Capacitance Measurements*: To evaluate the sensitivity and pressure range of the fabricated capacitive sensors, both electrodes were connected to the alligator clips of an LCR meter (ST2827A, Sourcetrionics, Germany) with copper tape. We used a mechanical tester (TA.XTplus, Stable Micro Systems, UK) with a 10 mm diameter cylindrical probe to apply pressure on the sensor. A small piece of Ecoflex 00-50 (Smooth-On Inc., USA) was placed on the probe tip to mimic tissue-like force source. The measurement setup is shown in Fig. 2.

In each experiment, the mechanical tester lowered the probe in contact with the sensor until a predetermined pressure (force divided by the probe surface area) was reached. The probe was held steady for a given contact time (0 s or 10 s, depending on the experiment), after which the load was removed. Pressures ranging from 0.1 to 50 kPa were tested. While different loads were being applied, the capacitance of the sensor was

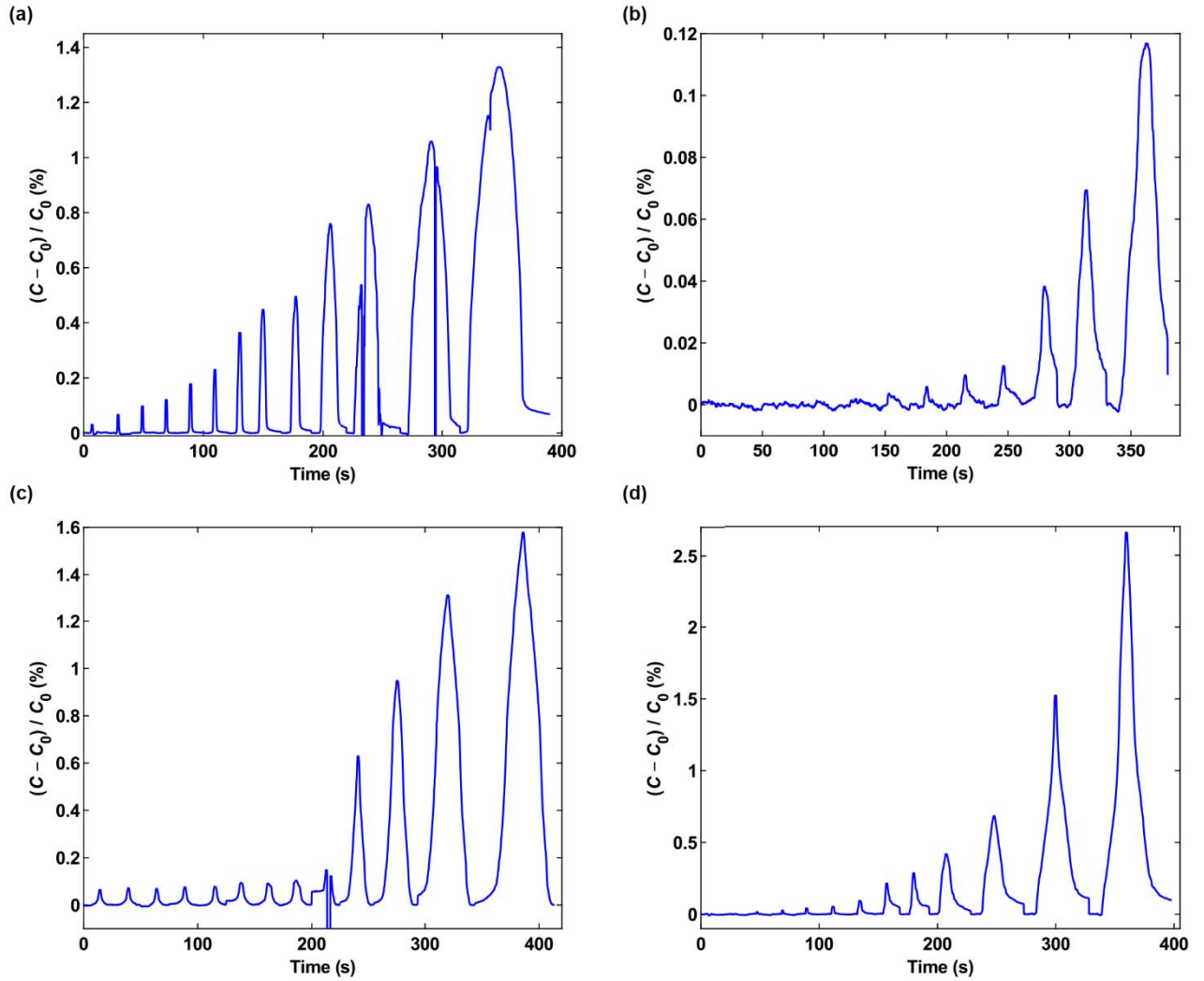


Fig. 5. Relative change in capacitance over time with different pressures from 0.1 kPa to 50 kPa (1 s load) for (a) softer PVA-PDMS sensor, (b) stiff PVA-PDMS sensor, (c) soft reference sensor, and (d) stiff reference sensor.

measured using the LCR meter, with a bias voltage of 1 V at a 10 kHz frequency.

The relative capacitance change  $\tilde{C}$  was calculated with:

$$\tilde{C} = \frac{C - C_0}{C}, \quad (2)$$

where  $C$  is the measured capacitance, and  $C_0$  is the initial capacitance at zero pressure. The sensitivity  $S$  of the sensor was calculated according to the following formula:

$$S = \frac{\Delta \tilde{C}}{\Delta P}, \quad (3)$$

where  $P$  is the applied pressure.

### III. RESULTS

#### A. Inkjet Printing Materials on PVA

The print resolution of the Ag NP ink was set to 770 dpi, and the printing parameters were optimized to allow the print to dry for 240 s before printing additional layers, and thus to avoid ink flooding. Ink drying was aided by keeping the plate temperature at 60 °C.

The electrical measurements showed that adding only a few layers of ink to the structure decreased the resistance of

the silver prints significantly (Fig. 3). The initial decrease is a lot faster than a simple inverse of the number of layers: the resistance of the 2-layer prints is only 20 % of the resistance of the 1-layer print. Additionally, the resistance values seemed to saturate at approximately 1-2  $\Omega/\square$  after 4-6 layers.

Furthermore, the mechanical toughness of the prints improved when higher ink volumes are used. The 1-layer prints were very fragile and tended to break after the dissolving of the PVA layer, but such behavior was not seen any more in the 2-layer prints. Based on these observations, we chose the 4-layer prints for further experiments.

The spreading of the PDMS ink was affected by the ink volume and drying time between layers. However, well-defined patterns could be obtained at an 876-dpi printing resolution, when a delay of 60 s was used between layers, and the plate temperature was kept at 60 °C.

To obtain a uniform dielectric, 4 layers of PDMS ink were jetted on the PVA film, resulting in an approximately 10  $\mu\text{m}$  thick dielectric layer. Even though the printed dielectric layer was rather thin, we observed it to be surprisingly convenient to handle with tweezers, at least in comparison

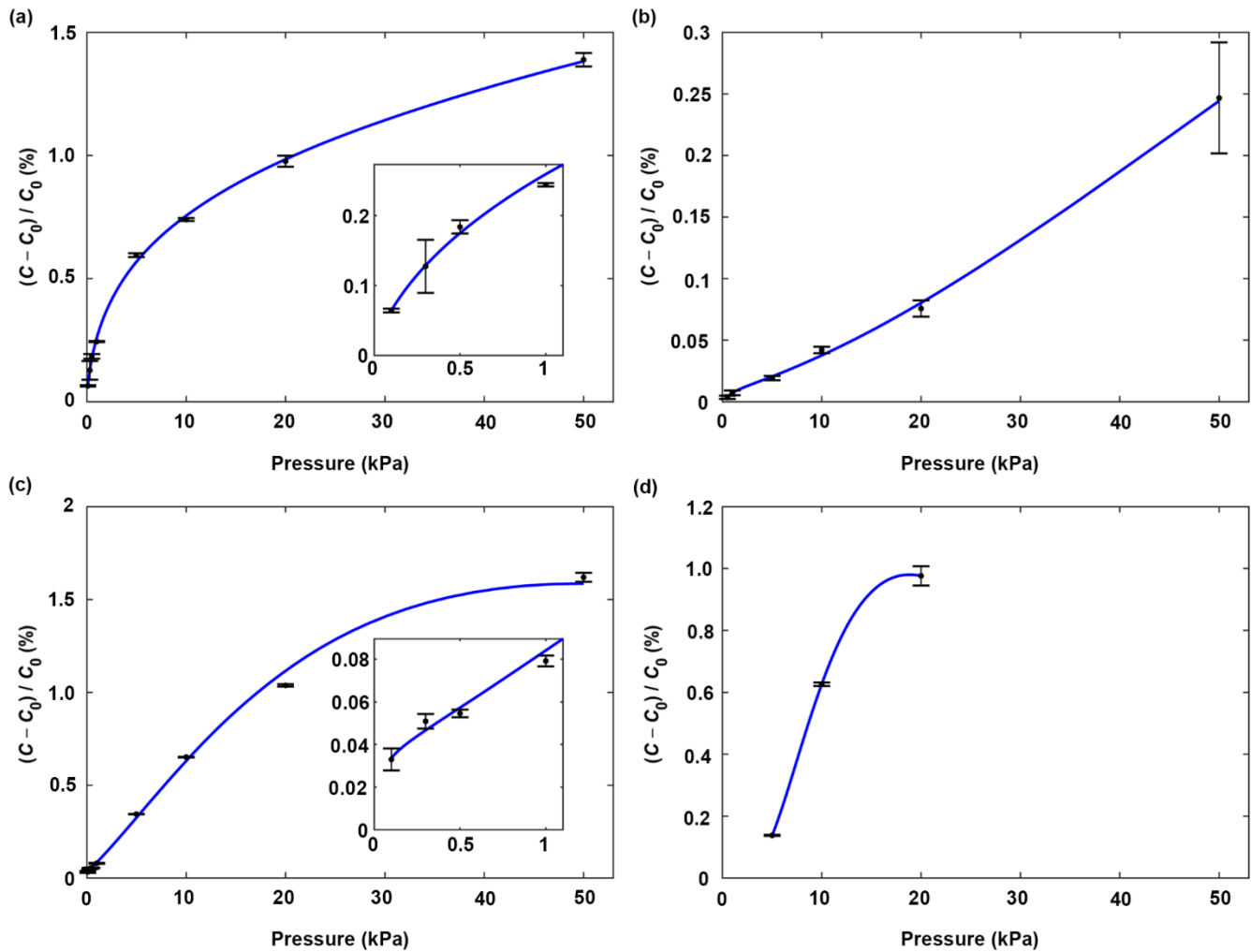


Fig. 6. Relative change in capacitance as a function of the applied pressures from 0.1 kPa to 50 kPa (10 s load) for (a) soft PVA-PDMS sensor, (b) stiff PVA-PDMS sensor, (c) soft reference sensor, (d) stiff reference sensor. Error bars show the standard deviation from the mean of 5 measurements.

to the spin-coated reference dielectric, despite the higher thickness of the latter (15  $\mu\text{m}$ ).

The stacked material layers of the sensors having either the spin-coated reference dielectric or the printed dielectric, are shown in Fig. 4. Both the surface SEM images, and cross-sectional images show that in the spin-coated version, the surface of the electrode (Fig. 4a) is more porous than that of the printed sensor (Fig. 4b). This is related to the fabrication process: since the bonding layer between the dielectric and the electrode is printed already before applying the electrode, the PDMS ink is penetrating the porous Ag NP mesh. In contrast, when the reference electrode is first attached to the dielectric, and the bonding layer is formed after that, the PDMS volume is smaller in the interface. This conclusion is supported by the cross-sectional images (Fig. 4c-f): although the mesh electrode in both sensor types is sponge-like, there are more cavities in the electrode of the reference sensor, even though traces of PDMS can be seen in this layer also.

The less porous composition of the printed mesh electrode is considered advantageous, since the electrode and the dielectric layer are more tightly attached to each other. It has been shown earlier, e.g. in [11], [35]–[37] that embedding the conductive material into PDMS is useful for the adhesion between the

material layers, and thus for the mechanical strength of the soft devices.

An interesting feature of the dielectric is seen in the cross-sectional images (Fig. 4c-f): the spin-coated dielectric has a uniform structure, whereas the printed dielectric is clearly porous. We assume this finding to correlate with the observed convenience of handling the printed PDMS foils: the PVA fibers are trapped inside the printed dielectric layer, and are therefore providing additional stiffness and mechanical support for the soft foils.

### B. Printed Tactile Sensors

The relative changes in the measured capacitance for each sensor as a function of time are shown in Fig. 5. The probe approached the sensor until the desired pressure was reached, and the load was maintained for 1 s, before the probe was retracted. The probe velocity was set to 0.1 mm/s during both approach and retraction. The applied pressures ranged from 0.1 kPa to 50 kPa.

Fig. 5 shows that the softer sensors (Figs 5a & c) can detect smaller pressures (<1 kPa) than the stiffer sensors (Fig. 5b & d). Furthermore, comparing the response of soft

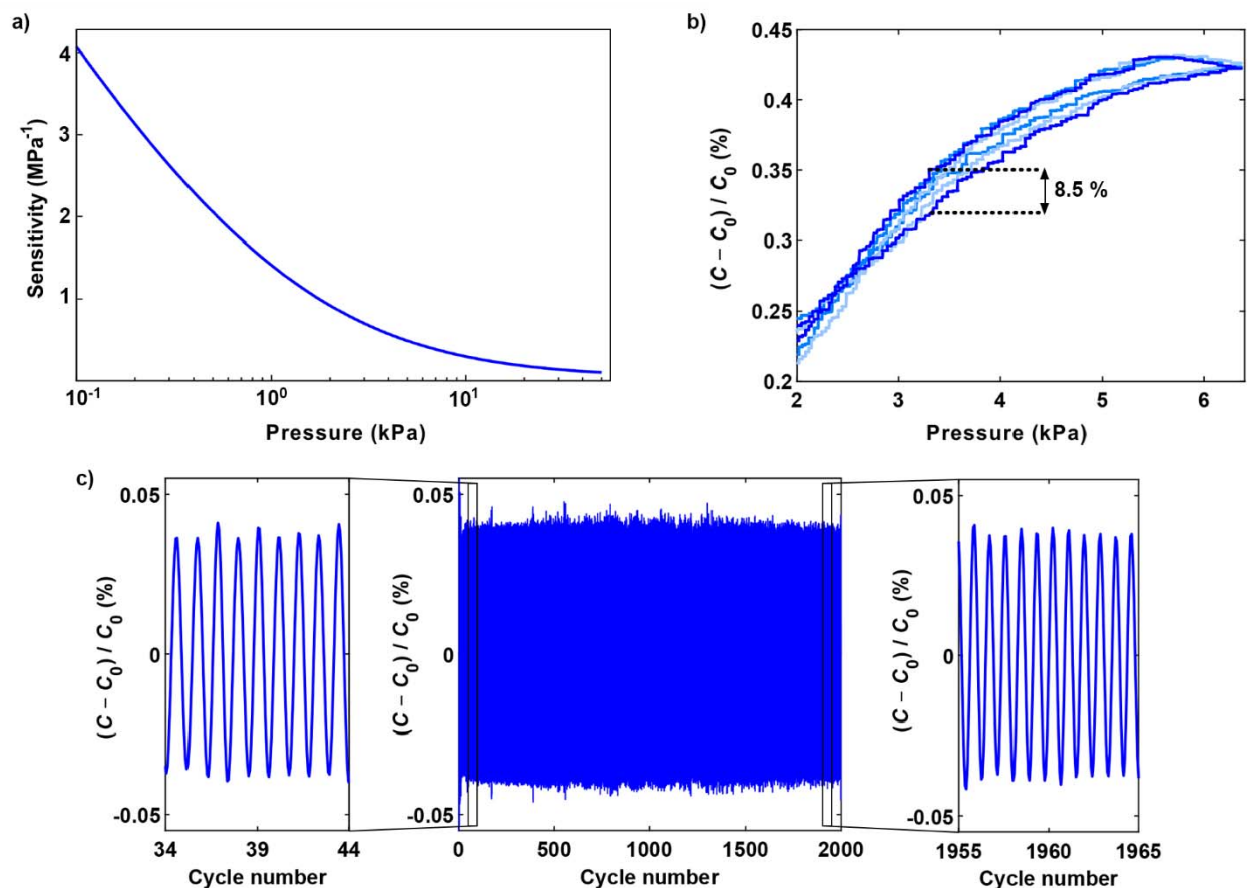


**Fig. 7.** a) The calculated sensitivity of the softer printed sensor as a function of applied pressure from 0.1 kPa to 50 kPa, b) the measured response and recovery of the sensor (2–6.4 kPa), maximum hysteresis of 8.5 % shown, c) sensor performance in a cyclic test, where a loading-unloading cycle was repeated for 2000 cycles at a frequency of 0.5 Hz.

PVA-PDMS sensor to the response of the soft reference dielectric sensor, we see that the reference dielectric sensor does not reliably recognize the difference between the applied pressures, until before the pressure reaches 5 kPa (Figs 5a & c).

The sudden changes in the signals of Fig. 5a (20 & 35 kPa) and Fig. 5c (5 kPa) may be a result from the probe mounting, irregularities in the mounting table surface, or other inevitable nonlinearities. It is also possible that the connectors bend under the applied pressure and could cause interference to the signal.

Overall, we take these observations as an evidence that the soft PVA-PDMS sensor has the most desirable pressure response, especially for applications where measuring small pressures is required. The sensitivity of the stiff printed sensor (Fig. 5b) seems to be approximately one-tenth of the measured sensitivities for the rest of the sensors. These results indicate that the presence of the PVA fibers in the dielectric stiffens the dielectric, improving the response of the soft elastomer layer, but diminishing the sensitivity of the already stiff dielectric, especially at low pressures. The stiff reference sensor shows great sensitivity at the largest pressures but is not capable to detect the low pressures as well as the softer ones.

To further study the pressure response of the sensors, we measured the capacitance while the sensors were pressed for 10 s with different pressures varying from 0.1 kPa to 50 kPa. The measurements were repeated at least four times. The results are shown in Fig. 6, where the relative change in

capacitance versus the applied pressure is shown for each sensor type. The stiff reference dielectric sensor broke during the experiments, so the Fig. 6 only shows the portion of measurements completed before the catastrophic failure of the sensor.

In Fig. 6, it can be noticed that the soft PVA-PDMS and the soft reference sensors have a sub-linear response, their sensitivity decreasing with the increment of the applied pressure, while the stiff PDMS-PVA sensor showed a more linear response. For many applications, such a sub-linear response is desirable: it allows distinguishing between small pressures accurately, while the decreasing sensitivity allows also measuring larger pressures.

Of the sensors tested, the soft PVA-PDMS has the highest sensitivity in the small pressure range. Therefore, we calculated the sensitivity for the soft PVA-PDMS sensor, and it is shown in Fig. 7a. The highest sensitivity ( $4 \text{ MPa}^{-1}$ ) was achieved with the smallest pressures (0.1 kPa) and this further confirms that the soft PVA-PDMS sensor is suitable for measuring small pressures.

To further study the performance of this sensor, we measured its hysteresis by consecutively applying a load on the sensor and then removing the load. Maximum load applied was 6.4 kPa. In these experiments, the probe speed was set very slow (0.01 mm/s), to avoid dynamic effects from, e.g., viscoelasticity of the materials. The results are shown in Fig. 7b. The hysteresis of the soft PVA-PDMS sensor is low ( $\leq 8.5\%$ ) in the measured pressure range. Here, the measured

relative change in capacitance is presented as a function of pressure varying from 2 kPa to approx. 6.4 kPa. With smaller pressures (0–2 kPa), the force probe was not pressing the thin sensor evenly, causing severe signal interference, and the response in that area was therefore discarded from further analysis. Based on these results, we conclude that the sensor has a small, but not insignificant hysteresis, which should be considered in the practical applications of these sensors.

To study the long-term stability of the sensor, we conducted a cyclic experiment, where the probe was set to move sinusoidally up and down to apply load on the sensor. The frequency of the probe was 0.5 Hz. The experiment was conducted so that first a static load was applied on the sensor and then the amplitude of the sinusoidal displacement was chosen so that the load varied approximately 20 kPa peak-to-peak. This cycle was repeated for 2000 times, and the obtained capacitance data were band-pass filtered (lower half-power frequency 0.35 Hz, higher half-power frequency 0.65 Hz) for a better presentation of the dynamic response.

The results of this experiment are presented in Fig. 7c. As seen in Fig. 7c, the printed soft PVA-PDMS sensor can detect the dynamic pressure variation accurately even after 2000 cycles. Based on these results from cyclic experiments, we conclude that the sensor can work reliably and repeatably for long periods of time.

To demonstrate a practical application of our sensors, we attached one of the printed soft sensors to a glove-covered fingertip and recorded the capacitance of the sensor while the finger was touching the underlying surface with varying pressures and hold times. As seen in the recorded video (S1), the sensor can detect the physical interaction with the surrounding environment.

#### IV. CONCLUSION

We have developed here a straightforward method for inkjet printing of PDMS based, multilayered electronics. This method is based on material printing on a temporary, supportive PVA layer that is first used to make mesh-like conductive layers, and to tune the properties of the elastomer dielectric, without the need for complex processing or hazardous chemicals. The applicability of this method for fabrication of soft devices was demonstrated by creating tactile pressure sensors.

The results show that this approach can improve the sensor performance significantly: small pressures (<1 kPa) can be detected accurately, and the fabricated sensors can detect pressures still at 50 kPa. This range covers most activities of the skin-like systems [38]. Moreover, low hysteresis ( $\leq 8.5\%$ ) and long-term repeatability over 2000 cycles were obtained. We also demonstrated here the suitability of these devices for tactile sensing by using them to detect fingertip's physical interaction with its surroundings. Furthermore, the additive and digital nature of the process allows both rapid prototyping and tuning of different sensor configurations. Therefore, our work paves way towards low-cost and easily customizable soft electronics with applications in, for example, wearable devices and smart prosthetics.

#### ACKNOWLEDGMENT

The authors would like to thank Teija Joki for her participation in the electrospinning process. They would also like to thank Mari Honkanen and Turkka Salminen for their contributions with sample preparation and execution of the cross-sectional imaging. This work made use of Tampere Microscopy Center Facilities at Tampere University.

#### REFERENCES

- [1] L. Zhou, J. Fu, Q. Gao, P. Zhao, and Y. He, "All-printed flexible and stretchable electronics with pressing or freezing activatable liquid-metal-silicone inks," *Adv. Funct. Mater.*, vol. 30, no. 3, Jan. 2020, Art. no. 1906683, doi: [10.1002/adfm.201906683](https://doi.org/10.1002/adfm.201906683).
- [2] Y. Chen *et al.*, "Shape-adaptive, self-healable triboelectric nanogenerator with enhanced performances by soft solid-solid contact electrification," *ACS Nano*, vol. 13, no. 8, pp. 8936–8945, Jul. 2019, doi: [10.1021/acsnano.9b02690](https://doi.org/10.1021/acsnano.9b02690).
- [3] J. Kim, B. Kang, and K. Cho, "Heat-assisted photoacidic oxidation method for tailoring the surface chemistry of polymer dielectrics for low-power organic soft electronics," *Adv. Funct. Mater.*, vol. 29, no. 11, Mar. 2019, Art. no. 1806030, doi: [10.1002/adfm.201806030](https://doi.org/10.1002/adfm.201806030).
- [4] L. Zhu, B. Wang, S. Handschuh-Wang, and X. Zhou, "Liquid metal-based soft microfluidics," *Small*, vol. 16, no. 9, Mar. 2020, Art. no. 1903841, doi: [10.1002/sml.201903841](https://doi.org/10.1002/sml.201903841).
- [5] Y. Shi, C. Wang, Y. Yin, Y. Li, Y. Xing, and J. Song, "Functional soft composites as thermal protecting substrates for wearable electronics," *Adv. Funct. Mater.*, vol. 29, no. 45, Nov. 2019, Art. no. 1905470, doi: [10.1002/adfm.201905470](https://doi.org/10.1002/adfm.201905470).
- [6] Y. Wang *et al.*, "Tough but self-healing and 3D printable hydrogels for E-skin, E-noses and laser controlled actuators," *J. Mater. Chem. A*, vol. 7, no. 43, pp. 24814–24829, Nov. 2019, doi: [10.1039/C9TA04248B](https://doi.org/10.1039/C9TA04248B).
- [7] H. Shi *et al.*, "Screen-printed soft capacitive sensors for spatial mapping of both positive and negative pressures," *Adv. Funct. Mater.*, vol. 29, no. 23, Jun. 2019, Art. no. 1809116, doi: [10.1002/adfm.201809116](https://doi.org/10.1002/adfm.201809116).
- [8] L. Lo, H. Shi, H. Wan, Z. Xu, X. Tan, and C. Wang, "Inkjet-printed soft resistive pressure sensor patch for wearable electronics applications," *Adv. Mater. Technol.*, vol. 5, no. 1, Jan. 2020, Art. no. 1900717, doi: [10.1002/admt.201900717](https://doi.org/10.1002/admt.201900717).
- [9] J. Jiang *et al.*, "Flexible piezoelectric pressure tactile sensor based on electrospun BaTiO<sub>3</sub>/poly(vinylidene fluoride) nanocomposite membrane," *ACS Appl. Mater. Interfaces*, vol. 12, no. 30, pp. 33989–33998, Jul. 2020, doi: [10.1021/acami.0c08560](https://doi.org/10.1021/acami.0c08560).
- [10] V. Vivekananthan, A. Chandrasekhar, N. R. Alluri, Y. Purusothaman, and S.-J. Kim, "A highly reliable, impervious and sustainable triboelectric nanogenerator as a zero-power consuming active pressure sensor," *Nanoscale*, vol. 2, no. 2, pp. 746–754, Feb. 2020, doi: [10.1039/C9NA00790C](https://doi.org/10.1039/C9NA00790C).
- [11] S. Kang *et al.*, "Highly sensitive pressure sensor based on bio-inspired porous structure for real-time tactile sensing," *Adv. Electron. Mater.*, vol. 2, no. 12, Dec. 2016, Art. no. 1600356, doi: [10.1002/aeml.201600356](https://doi.org/10.1002/aeml.201600356).
- [12] M. Han, J. Lee, J. K. Kim, H. K. An, S.-W. Kang, and D. Jung, "Highly sensitive and flexible wearable pressure sensor with dielectric elastomer and carbon nanotube electrodes," *Sens. Actuators A, Phys.*, vol. 305, Apr. 2020, Art. no. 111941, doi: [10.1016/j.sna.2020.111941](https://doi.org/10.1016/j.sna.2020.111941).
- [13] S. R. A. Ruth, L. Beker, H. Tran, V. R. Feig, N. Matsuhisa, and Z. Bao, "Rational design of capacitive pressure sensors based on pyramidal microstructures for specialized monitoring of biosignals," *Adv. Funct. Mater.*, vol. 30, no. 29, Jul. 2020, Art. no. 1903100, doi: [10.1002/adfm.201903100](https://doi.org/10.1002/adfm.201903100).
- [14] J.-H. Kim, S.-R. Kim, H.-J. Kil, Y.-C. Kim, and J.-W. Park, "Highly conformable, transparent electrodes for epidermal electronics," *Nano Lett.*, vol. 18, no. 7, pp. 4531–4540, Jul. 2018, doi: [10.1021/acs.nanolett.8b01743](https://doi.org/10.1021/acs.nanolett.8b01743).
- [15] D. E. Backman, B. L. LeSavage, S. B. Shah, and J. Y. Wong, "A robust method to generate mechanically anisotropic vascular smooth muscle cell sheets for vascular tissue engineering," *Macromolecular Biosci.*, vol. 17, no. 6, Jun. 2017, Art. no. 1600434, doi: [10.1002/mabi.201600434](https://doi.org/10.1002/mabi.201600434).
- [16] M. P. Drupitha *et al.*, "Morphology-induced physico-mechanical and biological characteristics of TPU-PDMS blend scaffolds for skin tissue engineering applications," *J. Biomed. Mater. Res. B. Appl. Biomater.*, vol. 107, no. 5, pp. 1634–1644, Jul. 2019, doi: [10.1002/jbm.b.34256](https://doi.org/10.1002/jbm.b.34256).

- [17] X. Shuai *et al.*, “Highly sensitive flexible pressure sensor based on silver nanowires-embedded polydimethylsiloxane electrode with microarray structure,” *ACS Appl. Mater. Interfaces*, vol. 9, no. 31, pp. 26314–26324, Jul. 2017, doi: [10.1021/acsami.7b05753](https://doi.org/10.1021/acsami.7b05753).
- [18] J. Hwang, S. G. Lee, S. Kim, J. S. Kim, D. H. Kim, and W. H. Lee, “Unveiling viscoelastic response of capacitive-type pressure sensor by controlling cross-linking density and surface structure of elastomer,” *ACS Appl. Polym. Mater.*, vol. 2, no. 6, pp. 2190–2198, May 2020, doi: [10.1021/acsapm.0c00193](https://doi.org/10.1021/acsapm.0c00193).
- [19] Y. Kim, S. Jang, and J. H. Oh, “Fabrication of highly sensitive capacitive pressure sensors with porous PDMS dielectric layer via microwave treatment,” *Microelectronic Eng.*, vol. 215, Jul. 2019, Art. no. 111002, doi: [10.1016/j.mee.2019.111002](https://doi.org/10.1016/j.mee.2019.111002).
- [20] E. Thouti *et al.*, “Tunable flexible capacitive pressure sensors using arrangement of polydimethylsiloxane micro-pyramids for bio-signal monitoring,” *Sens. Actuators A, Phys.*, vol. 314, Oct. 2020, Art. no. 112251, doi: [10.1016/j.sna.2020.112251](https://doi.org/10.1016/j.sna.2020.112251).
- [21] L. Ma *et al.*, “A highly sensitive and flexible capacitive pressure sensor based on a micro-arranged polydimethylsiloxane dielectric layer,” *J. Mater. Chem. C*, vol. 6, no. 48, pp. 13232–13240, Dec. 2018, doi: [10.1039/C8TC04297G](https://doi.org/10.1039/C8TC04297G).
- [22] X. Zeng *et al.*, “Tunable, ultrasensitive, and flexible pressure sensors based on wrinkled microstructures for electronic skins,” *ACS Appl. Mater. Interfaces*, vol. 11, no. 23, pp. 21218–21226, May 2019, doi: [10.1021/acsami.9b02518](https://doi.org/10.1021/acsami.9b02518).
- [23] V. Palaniappan *et al.*, “Laser-assisted fabrication of a highly sensitive and flexible micro pyramid-structured pressure sensor for E-skin applications,” *IEEE Sensors J.*, vol. 20, no. 14, pp. 7605–7613, Jul. 2020, doi: [10.1109/JSEN.2020.2989146](https://doi.org/10.1109/JSEN.2020.2989146).
- [24] X. Wang *et al.*, “Printed conformable liquid metal e-skin-enabled spatiotemporally controlled bioelectromagnetics for wireless multisite tumor therapy,” *Adv. Funct. Mater.*, vol. 29, no. 51, Dec. 2019, Art. no. 1907063, doi: [10.1002/adfm.201907063](https://doi.org/10.1002/adfm.201907063).
- [25] P. Wei *et al.*, “Flexible and stretchable electronic skin with high durability and shock resistance via embedded 3D printing technology for human activity monitoring and personal healthcare,” *Adv. Mater. Technol.*, vol. 4, no. 9, Sep. 2019, Art. no. 1900315, doi: [10.1002/admt.201900315](https://doi.org/10.1002/admt.201900315).
- [26] S. Mashihi *et al.*, “A novel printed fabric based porous capacitive pressure sensor for flexible electronic applications,” in *Proc. IEEE SENSORS*, Oct. 2019, pp. 1–4, doi: [10.1109/SENSORS43011.2019.8956672](https://doi.org/10.1109/SENSORS43011.2019.8956672).
- [27] S. Wang *et al.*, “Skin electronics from scalable fabrication of an intrinsically stretchable transistor array,” *Nature*, vol. 555, no. 7694, p. 83, 2018, doi: [10.1038/nature25494](https://doi.org/10.1038/nature25494).
- [28] M. Tavakoli *et al.*, “EGaIn-assisted room-temperature sintering of silver nanoparticles for stretchable, inkjet-printed, thin-film electronics,” *Adv. Mater.*, vol. 30, no. 29, Jul. 2018, Art. no. 1801852, doi: [10.1002/adma.201801852](https://doi.org/10.1002/adma.201801852).
- [29] M. Su *et al.*, “Nanoparticle based curve arrays for multirecognition flexible electronics,” *Adv. Mater.*, vol. 28, no. 7, pp. 1369–1374, Feb. 2016, doi: [10.1002/adma.201504759](https://doi.org/10.1002/adma.201504759).
- [30] R. Mikkonen, P. Puustola, I. Jönkkäri, and M. Mäntysalo, “Inkjet-printable polydimethylsiloxane for all-inkjet-printed multilayered soft electrical applications,” *ACS Appl. Mater. Interfaces*, vol. 12, no. 10, pp. 11990–11997, 2020, doi: [10.1021/acsami.9b19632](https://doi.org/10.1021/acsami.9b19632).
- [31] R. Mikkonen and M. Mäntysalo, “Inkjettable, polydimethylsiloxane based soft electronics,” in *Proc. IEEE Int. Conf. Flexible Printable Sensors Syst. (FLEPS)*, Aug. 2020, pp. 1–3, doi: [10.1109/FLEPS49123.2020.9239558](https://doi.org/10.1109/FLEPS49123.2020.9239558).
- [32] A. Miyamoto *et al.*, “Inflammation-free, gas-permeable, lightweight, stretchable on-skin electronics with nanomeshes,” *Nature Nanotechnol.*, vol. 12, no. 9, pp. 907–913, Sep. 2017, doi: [10.1038/nnano.2017.125](https://doi.org/10.1038/nnano.2017.125).
- [33] S. Lee *et al.*, “Nanomesh pressure sensor for monitoring finger manipulation without sensory interference,” *Science*, vol. 370, no. 6519, pp. 966–970, Nov. 2020, doi: [10.1126/science.abc9735](https://doi.org/10.1126/science.abc9735).
- [34] Y. Wang *et al.*, “A durable nanomesh on-skin strain gauge for natural skin motion monitoring with minimum mechanical constraints,” *Sci. Adv.*, vol. 6, no. 33, Aug. 2020, Art. no. eabb7043, doi: [10.1126/sciadv.abb7043](https://doi.org/10.1126/sciadv.abb7043).
- [35] Q. Huang, K. N. Al-Milaji, and H. Zhao, “Inkjet printing of silver nanowires for stretchable heaters,” *ACS Appl. Nano Mater.*, vol. 1, no. 9, pp. 4528–4536, Aug. 2018, doi: [10.1021/acsanm.8b00830](https://doi.org/10.1021/acsanm.8b00830).
- [36] K.-H. Jung, J. Kim, B.-G. Park, C.-J. Lee, H.-J. Sung, and S.-B. Jung, “Fabrication of a circuit embedded in PDMS substrate and its mechanical and electrical property with variations of photonic energy,” *J. Alloys Compounds*, vol. 748, pp. 898–904, Jun. 2018, doi: [10.1016/j.jallcom.2018.03.171](https://doi.org/10.1016/j.jallcom.2018.03.171).
- [37] H. Fan *et al.*, “Prepolymerization-assisted fabrication of an ultrathin immobilized layer to realize a semi-embedded wrinkled AgNW network for a smart electrothermal chromatic display and actuator,” *J. Mater. Chem. C*, vol. 5, no. 37, pp. 9778–9785, 2017, doi: [10.1039/C7TC03358C](https://doi.org/10.1039/C7TC03358C).
- [38] Y. Zang, F. Zhang, C.-A. Di, and D. Zhu, “Advances of flexible pressure sensors toward artificial intelligence and health care applications,” *Mater. Horizons*, vol. 2, no. 2, pp. 140–156, 2015, doi: [10.1039/C4MH00147H](https://doi.org/10.1039/C4MH00147H).



**Riikka Mikkonen** received the B.Sc. and M.Sc. degrees in electrical engineering from the Tampere University of Technology, Tampere, Finland, in 2015 and 2017, respectively. She is currently pursuing the D.Sc. degree in electronics with Tampere University, Tampere. Her research interests include printed electronics, especially printable materials, and their applications for soft and flexible devices.



**Anastasia Koivikko** received the B.Sc. and M.Sc. degrees in biomedical engineering from the Tampere University of Technology, Tampere, Finland, in 2015 and 2017, respectively, where she is currently pursuing the D.Sc. degree. In 2019, she worked a Guest Researcher with the Max Planck Institute for Intelligent Systems. Her research interests include fabrication of soft robots, especially soft grippers and integration of stretchable sensors into soft robotic systems.



**Tiina Vuorinen** received the B.Sc. and M.Sc. degree in electrical engineering from the Tampere University of Technology, Tampere, Finland, in 2013 and 2014, respectively. She is currently pursuing the D.Sc. degree in electronics with Tampere University, Tampere. Her research interests include printed electronics, materials in electronics and conformable electronics.



**Veikko Sariola** (Member, IEEE) received the D.Sc. (Tech.) degree in electrical engineering from Aalto University, Finland, in 2012. From 2013 to 2015, he was a Postdoctoral Researcher with Carnegie Mellon University. In 2016, he was appointed as a Research Fellow from the Academy of Finland. He is currently an Associate Professor of Biomedical Microsystems with Tampere University, Finland. His current research interests include bio-inspired materials and robotics.



**Matti Mäntysalo** (Member, IEEE) received the M.Sc. and D.Sc. (Tech.) degrees in electrical engineering from the Tampere University of Technology, Tampere, Finland, in 2004 and 2008, respectively. From 2011 to 2012, he was a Visiting Scientist with the iPack Vinn Excellence Center, School of Information and Communication Technology, KTH Royal Institute of Technology, Stockholm, Sweden. He is currently a Professor of Electronics Materials and Manufacturing with Tampere University. His current research interests include printed electronics materials, fabrication processes, stretchable electronics, and especially the integration of printed electronics with silicon-based technology (hybrid systems). He was a recipient of the Academy Research Fellow Grant from the Academy of Finland from 2015 to 2020.